Protection of W7-X diagnostics from radiation heat loads

André Carls[*], Matthias Köppen, Joris Fellinger, Felix Schauer

Max Planck Institute for Plasma Physics, EURATOM Association, Wendelsteinstr. 1, 17491 Greifswald, Germany

Abstract

Wendelstein 7-X (W7-X), a modular advanced stellarator, is presently under construction at the Max Planck Institute for Plasma Physics in Greifswald. Part of the inner plasma vessel (PV) surface is covered by graphite tiles which are bolted onto water-cooled CuCrZr heat sink plates. This so-called heat shield shall protect in-vessel components and the PV wall from plasma-edge-radiation and convective heat loads. Numerous diagnostics (e.g. Diamagnetic loops , Rogowski coils, etc.) are located in between the heat shield and plasma vessel wall. They are loaded by thermal radiation from the hot heat shield backside, stray radiation from the electron cyclotron resonance heating (ECRH), and plasma radiation through remaining gaps between the tiles. In order to keep the temperatures of the diagnostics within their specified limits, additional shielding is required. The paper presents the design of such a shielding for the diamagnetic loops and Rogowski coils. Several options of copper shields and loosely attached Sigraflex®-layers, and combinations thereof, are compared with respect to their abilities to reduce the temperatures of the sensitive parts of the diagnostics. To increase the confidence in the results, a sensitivity study with widely varying radiative material properties has been carried out. The advantages and disadvantages of the potential solutions are discussed. As a result two copper shield variants which also reduce the load onto the plasma vessel are presented.

[*]corresponding author

1 Introduction

The W7-X plasma vessel and diagnostics are protected by the heat shield or first wall, consisting of graphite tiles mounted on CuCrZr heat sinks (see Figure 2). The thermal load on the first wall was initially assumed to be about 200...300 kW·m^{-2} [1, 2]. Later studies showed that in spatially limited regions loads on the first wall attain up to 500 kW·m^{-2}. The water cooled heat sinks remove only part of the thermal energy from the graphite tiles. Their hot backsides emit the remaining heat to the plasma vessel, intermediary components and diagnostics, as shown in section (A) of Figure 3. This heat load is increased by the homogeneously dirstibuted ECRH stray radiation. Mock-up tests of diagnostics showed that the W7-X ECRH design load of 50 kW·m^{-2} generated temperatures close to or above 250 ℃ for certain diagnostics in the Microwave Stray Radiation Loading Facility (MISTRAL) [3]. This is a hazardous situation due to the temperature limit of 250 ℃ for diagnostics with Kapton® insulated wires. The heat flux on the plasma vessel reaches up to 15 kW·m^{-2} which significantly exceeds the design value of about 2 kW·m^{-2} [6] (see Figure 1). The paper presents shielding options to reduce the load on the plasma vessel and diagnostics. First a rough estimate is performed to choose a basic shield concept which is developed and analysed in the consecutive sections. Two shield variants are shown to be suitable to reduce the loads on diagnostics and plasma vessel to acceptable values.

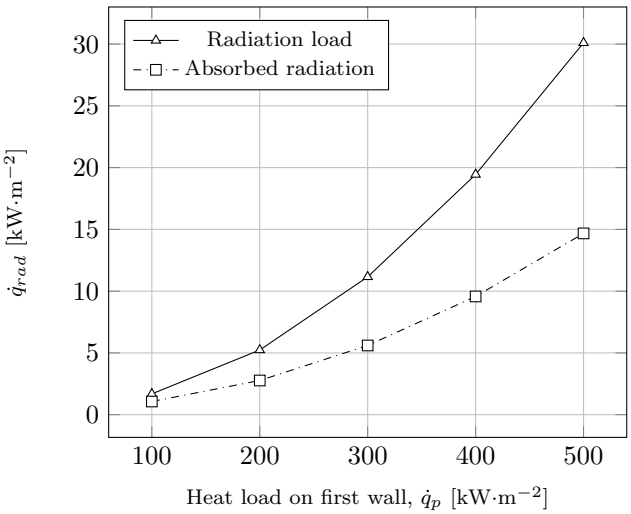

Figure 1: Emitted radiation from the backside of the first wall plus ECRH stray radiation and absorbed radiation on the plasma vessel.

2 Choice of shield concept

Heat load reduction can be achieved by installing a radiation heat shield behind the first wall and/or by reduction of ECRH heat fluxes with help of absorbing coatings. Last point is a discussed option, but the application seems not to be practical.

Thus only thermal radiation shields were considered: extension of the Sigraflex®-layer between graphite and CuCrZr, and insertion of additional reflecting Cu-sheets as shown in Figure 3. An estimation for radiation loads through such a shield in between the first wall and the plasma vessel was done using the relation

$$\dot{q}_{rad} = \frac{\sigma\left(T_{fw}^4 - T_{PV}^4\right)}{\frac{1}{\epsilon_{fw}} + \frac{1}{\epsilon_{PV}} - 1 + \left(\frac{2}{\epsilon_{shield}} - 1\right)} \qquad (1)$$

from literature [4]. The average backside temperature for the first wall was evaluated by taking the mean over the heat load portions emitted by the CuCrZr and graphite surfaces. This yields

$$T_{fw} = \sqrt[4]{\frac{1}{\sigma\epsilon_{fw}} \cdot \frac{\sum\left(A_i T_i^4\right)}{\sum A_i}}, \qquad (2)$$

where σ is the Stefan-Boltzmann-constant and ϵ_{fw}, the average emissivity of the backside. The fact that 85% of the emitted heat originates from the graphite tiles is taken into account by an emissivity of $\epsilon_{fw} = 0.9$ for the first wall. The average temperature for the highly loaded first wall backside is then $T_{fw,500} = 590$ ℃, whereas for the normally loaded tiles the temperature evaluates to $T_{fw,250} = 345$ ℃. The plasma vessel temperature was assumed to be

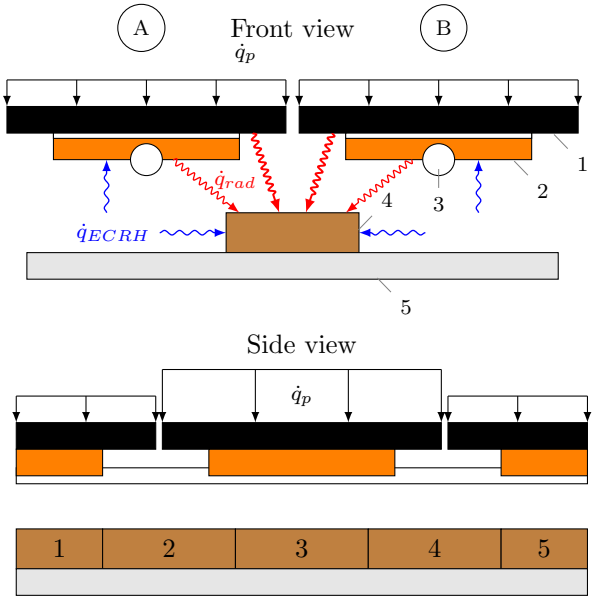

Figure 2: Cross section of the heat-shield area with subjacent diagnostics. ***top)*** (A) shows the situation without additional protection: Heat loads ($\dot{q}_p$) from the plasma hit the heat-shield. The heat diffuses through the graphite tiles (1) into the CuCrZr heat sink (2), both connected via a 1 mm thick Sigraflex®-layer in between. Heat is then absorbed by the water cooling (3). Diagnostics (4) are heated by thermal radiation ($\dot{q}_{rad}$) from the backside of the first wall and EC-stray radiation ($\dot{q}_{ECRH}$). The same applies for the Plasma Vessel (5). ***bottom)*** The side view shows the segments of the Diamagnetic loop diagnostic below the first wall and the spatial distribution of the peak load in poloidal direction.

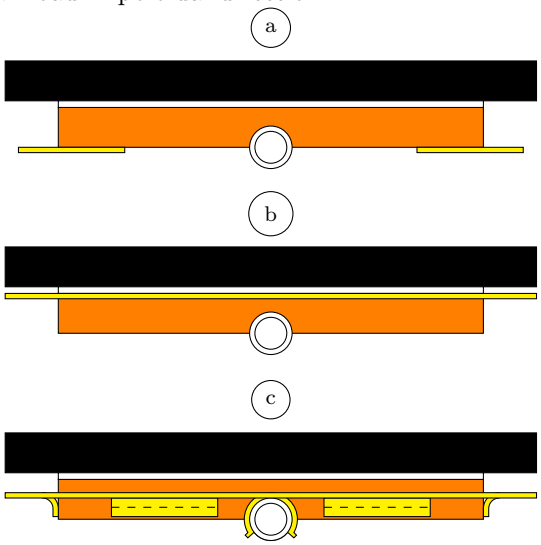

Figure 3: Options for the radiation shield below the first wall tiles. ***a)*** A Cu-shield mounted on the bottom side of the CuCrZr heat sink. ***b)*** Cu-sheet installed below the first wall tile and before CuCrZr.

$T_{PV} = 60$ °C with an emissivity of $\epsilon_{PV} = 0.5$. These numbers show the dependency of the backside temperature on the $A_{Graphite}/A_{CuCrZr}$ ratio (c.f. [5]).

The heat loads for a 2×3 tile array of the first wall were also evaluated. It was obtained by $\dot{q}_{rad,array} = (2\dot{q}_{rad,250} + \dot{q}_{rad,500})/3$ because it consists of two highly loaded tiles and four normally loaded tiles. It turned out that a Sigraflex®-layer was not worth to be considered further. As listed in Table 1 it reduces the radiation heat flux density only by 40%, whereas an ideal Cu-shield reduces the heat flux density by 70%. Subsequently only a Cu-shield was considered. The estimate is conservative since the Cu-shields as discussed in the following sections are contacted to the heat sink which reduces the heat flux further.

Option	$\dot{q}_{rad,500}$ [kW·m^{-2}]	$\dot{q}_{rad,250}$ [kW·m^{-2}]	$\dot{q}_{rad,array}$ [kW·m^{-2}]
Unprotected	14.8	3.6	7.3
Sigraflex®-layer	9.4	2.3	4.6
Cu-shield	4.5	1.1	2.2

Table 1: Estimated radiative heat flux density for highly loaded first wall tiles ($\dot{q}_{rad,500}$) and normally loaded tiles ($\dot{q}_{rad,250}$). The last column gives an estimation for the section of the later presented 3D model where highly and normally loaded tiles are considered in a 2×3 array.

3 Detailed investigation of the chosen concept

3.1 Design options

Three copper shield options are discussed in more detail: *a)* Cu-sheet either bolted below the heat sink or *b)* inserted between graphite tile and CuCrZr heat sink or *c)* a Cu-shield which is clamped onto the pipes, completely surrounding and touching the heat sink (see Figure 3). Detailed models of all versions were analyzed with FEA.

The thickness of the Cu-shield is 0.5 mm. Emis-

sivities for stainless steel (ss) and CuCrZr were assumed to be $\epsilon_{ss} = 0.5$, for copper $\epsilon_{Cu} = 0.35$ and for graphite $\epsilon_G = 0.9$. The ECRH absorbances are taken as $\alpha_{ss} = 1\%$, $\alpha_{CuCrZr} = 2\%$, $\alpha_G = 5\%$ and $\alpha_{Cu} = 0.3\%$ [9]. All models are built up on top of a 250×150 mm wide portion of the plasma vessel. Five segments of the Diamagnetic-loop connected via copper stripes to the plasma vessel, are considered in options *a* and *b*. The first wall is represented by six tiles, arranged in a 2×3 array. The center tiles were loaded with 500 kW·m^{-2}, whereas the remaining tiles with 250 kW·m^{-2} (see Figure Figure 4). An ECRH load of 50 kW·m^{-2} was applied to all surfaces.

3.2 Parametric studies

The exact radiative material properties and their change during future machine operation are unknown. The main mechanism influencing the radiation characteristics is carbon dust deposition. Studies on other machines showed that carbon dust deposition depends on the location within the plasma vessel and the distance from the plasma [7]. Dependencies of the surface reflectivity on the thickness of the carbon deposited layer make it even more uncertain [8]. Thus the full range of possible reflectance degradation for stainless steel was investigated (see Table 2). The same degradation was assumed for CuCrZr which is the dominating material at the backside of the first wall. Copper emissivity and stainless steel emissivities were varied within a similar relative range. The microwave absorption properties were varied within the limits of known uncertainties [9]. However, the large parameter range is no major concern because the contribution to the overall heat balance remains small.

4 Results

The installation of a Cu-shield significatnly decreases temperatures in subjacent diagnostics. In the example of the Diamagnetic loop the temperature drops from 330 ℃ to around 160 ℃ for the bolted Cu-shield (*a*) and for the Cu-sheet in between the tile and CuCrZr (*b*). The variation in the temperature of the diagnostics over the different options is small.

The radiative heat fluxes onto the plasma vessel were calculated for options *a* and *b* with the Diamanetic loop present, for option *c* without. The Diamanetic loop has only little influence on the plasma vessel load. Heat fluxes are reduced by a factor of about two with a bolted Cu-shield. A factor of around 2.5 can be reached for the two other options (see Figure 5). The lower efficiency of option *a* can be explained by the necessarily smaller shield dimensions which result in larger gaps for plasma radiation. Result details are given in Table 3. Remaining cumulative heat fluxes, from thermal and ECRH stray radiation with or without conductive terms from diagnostics, still persist on a level which is at the design limit. With the assumed level of ECRH absorption for the plasma vessel, one obtains values slightly above to 2 kW·m^{-2} (see Table 3).

From variation of the radiative properties ϵ and α a ΔT of around 50 K for the plasma vessel temperature and 70 K for the diagnostics was obtained (see Figure 6). Since the radiative loads on the components and the plasma vessel are the highest for the bolted Cu-shield, it can be concluded that ΔT for the other options is smaller.

5 Conclusions

Simple estimations of heat fluxes from the first wall to the plasma vessel showed the benefit of an additional Cu-shield behind the first wall. Accurate FEA calculations, considering thermal contact between the Cu shield and CuCrZr heat sink, confirmed the suitablity of options *b* (Cu-sheet between graphite tile and the CuCrZr) and *c* (Cu-shield surrounding and touching the heat sink). The radiation load on plasma vessel and diagnostics can be reduced by an amount of 70% or more.

As a consequence, the temperatures of the diagnostics can be kept at about 170 ℃, well below their limit of 250 ℃. Furthermore, it was demonstrated that possible temperature variations, based on different material properties and carbon deposition, cause temperature variations of about 70 K, which still leaves margins for diagnostic components.

Material	Emissivity, ϵ [-]	ECRH abs. coeff., α [%]
Cu	0.35...0.5 (.35)	0.1...0.3 (0.1)
CuCrZr	0.45...0.8 (0.5)	0.2
SS	0.45...0.8 (0.5)	1...3 (1)
Graphite	0.9	5

Table 2: Ranges for the parametric studies of the radiative properties. Standard values are noted in brackets.

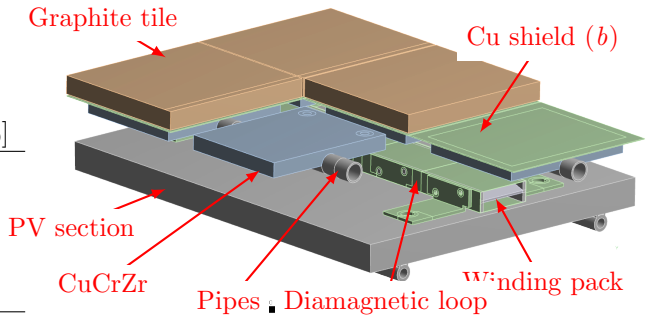

Figure 4: 3D model of design option b for the calculation of the heat flux density.

Option	$\dot{q}_{rad}$	$\dot{q}_c$	$\dot{q}_{ECRH}$	$\dot{q}_{tot}$ [kW·m^{-2}]
unprot.	2.94	1.36	0.5	4.8
a	2.0	0.67	0.5	3.2
b	1.15	0.75	0.5	**2.4**
c	1.7	–	0.5	**2.2**

Table 3: Cumulative heat fluxes on the plasma vessel for the detailed analysed options with standard values for ϵ and α. $\dot{q}_{tot}$ is the cumulative heat flux onto the plasma vessel, resulting from thermal conduction ($\dot{q}_c$) through attached diagnostics, net radiation ($\dot{q}_{rad}$) from the heat shield and ECRH stray radiation ($\dot{q}_{ECRH}$). The diagnostics were not considered in the analysis of type *c*.

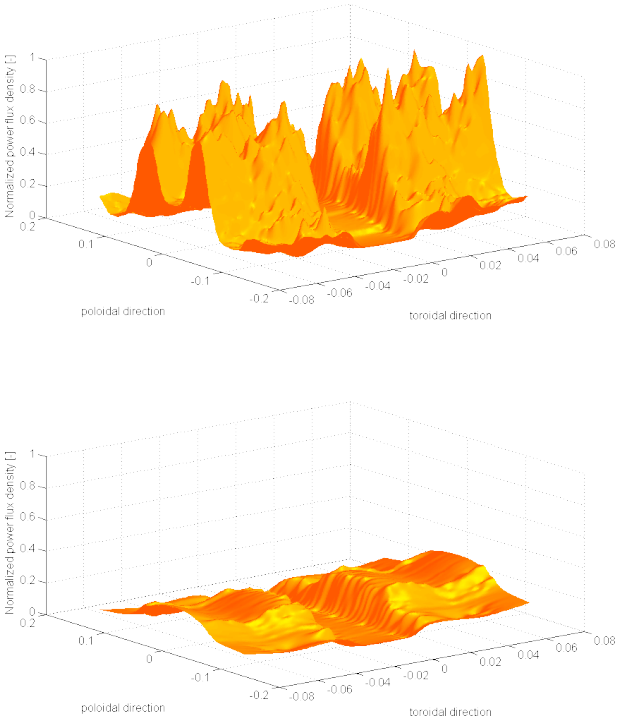

Figure 5: ***top)*** Normalized radiation heat flux density distribution for a section of the plasma vessel without shielding. Well to see is the Diamanetic loop in the center, shielding the vessel surface partially. To the left and right of the Diamanetic loop the slits between the heat shield section are good to identify, resulting in stretched peaks of incoming radiation. Sharp peaks arise from the discretization of the 3d-model. The heat flux density is normalized to the peak value of the unshielded portion. ***bottom)*** Radiation heat flux density distribution for design option *b*. The radiation through the slits disappears and only the part from the hot backside is left over.

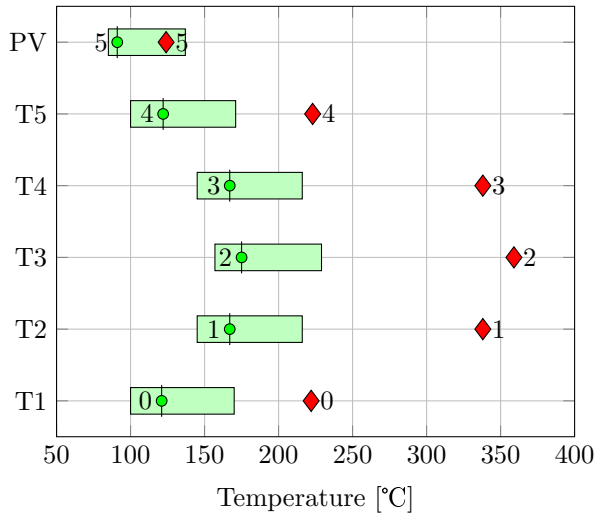

Figure 6: Bar plot of the calculated temperature ranges for option *a*. Temperature ranges for various segments of the Diamagnetic loop (T1,. . . ,T5, see Figure 2) and the plasma vessel (PV). Circles with a vertical bar indicate the standard values. Diamonds show the calculated temperatures for an unprotected Diamagnetic loop.

Not fully satisfying is the reduction of heat loads with respect to the plasma vessel, where with 2.2 kW·m^{-2} the design value is surpassed by about 10%. However, considering the conservative assumptions and thhe small hot spot extensions the result is still acceptable.

The shield options *b* and *c* are thus suitable choices for the solution of the problem.

References

[1] H. Greuner, *et. al.*, Concepts and prototype elements of the low-Z wall protection for the stellarator W7-X, Fus. Eng. and Des., Volumes 56-57 (2001) 297-302

[2] R. Stadler, *et. al.*, The in-vessel components of the experiment WENDELSTEIN 7-X, Fus. Eng. and Des., Volume 84, Issues 2-6 (2009) 305–308

[3] D. Hathiramani, *et al.*, Fus. Eng. and Des., this conference

[4] H.D. Baehr, K. Stephan, Wärme- und Stoffübertragung, Springer-Verlag, Berlin, 1998

[5] X.B. Peng, *et. al.*, Thermo-mechanical analysis of Wendelstein 7-X plasma facing components, Fus. Eng. and Des., this conference

[6] M. Nagel, *et. al.*, Thermal and structural analysis of the W7-X magnet heat radiation shield, Fus. Eng. and Des., Volumes 75-79 (2005) 139–142

[7] V.S. Voitsenya, A. Sagara, A.F. Bardamid, *et al.*, *et al.*, Effect of exposure inside the LHD vessel on reflectance of stainless steel mirrors, Problems of Atomic Science and Technology. (2002) "Plasma Physics" #5(8) 39-41

[8] K.Yu. Vukolov, *et al.*, The deposition of contaminants on the in-vessel mirrors in T-10 tokamak, ECA Vol.28G, (2004)

[9] H. Laqua, Spezifikation für Mikrowellenstreustrahlung in W7-X, 1-CBD20-S0001.2, internal report (2010)